A Texture-based Approach to Chest Radiography Segmentation

Ha Dai Duong and Dao Thanh Tinh

Abstract— **Segmentation is an important pre-processing step for many inspections or detections in image analysis. This paper presents a new approach where we integrate statistical features in the segmentation process of chest radiography, which is the first step towards a computer-aided diagnosis system. In this proposal, instead of using the intensity of a given pixel, a statistical feature vector is extracted from a sliding window centred on the pixel, and then a multilevel threshold segmentation algorithm is applied. Experimental results are given to demonstrate the improved performance of the proposed method.**

Index: Chest radiography, computer-aided diagnosis, texture-based segmentation.

I. INTRODUCTION

Due to the importance role of computer-aided diagnostic (CAD) systems and the convenience, low cost and low radiation dose of chest radiographs [1], a variety of image processing and analysis methodologies for chest radiographs has been proposed. As the first step towards a CAD system, segmentation of plain chest radiographs has attracted some attention [2], many of them have focused on the segmentation of the lung fields, whereas fewer have focused on the segmentation of the rib cage or other anatomic structures of the chest [3], [4], [5], and in [6] an general purpose x-ray image segmentation based on clustering was introduced. Alexandros Karargyris et el. in [3] presented a novel approach for detecting lungs and ribs in chest radiographs. Their approach used region-based features computed as wavelet features, these took into consideration the orientation of anatomic structures; and classified non-rib lung regions for radiographic patterns suggesting tuberculosis infection. This work concentrated only on one of anatomic structures as such as the authors of [4] and [5]. Chhanda Ray and Krishnendu Sasmal in [6] presented a new method directed towards the automatic clustering of x-ray images. The clustering has been done based on multi-level feature of given x-ray images such as global level, local level and pixel level; however, since the dimensionality of feature space in this methods is huge and no dimensionality reduction is used, space complexity increases.

For the purpose of providing a medical image analysis technique, this work focuses on segmenting of chest radiographs into three intensity groups: dark, gray and light regions. In these groups, some part of gray region may be caused by disease. The intensity of a pixel in a radiographs depends principally on radiographic contrast of biological tissues [7]. The radiation attenuation properties of each tissue type in turn is determined by its elemental and chemical composition, as it is for all other chemical compounds and mixtures. In this discussion, we consider the body which consists of fat, (lean) soft tissue, bone, water and air (found in the lungs). Radiographic contrast refers to the difference in the number of x-ray photons emerging from adjacent regions of the object being scanned, which depends on differences in atomic number, physical density, electron density, thickness, as well as the energy spectrum of the x-ray beam emitted by the source. Radiographic contrast properties of body constituents are given in Table I, the table indicates that these constituents can divide into three or four groups.

TABLE I

PHYSICAL PROPERTIES OF HUMAN BODY CONSTITUENTS

Material	Effective $AtomicNo.$	Density (gm/cm^3)	Electron density $(electrons/kg)$
Air	7.6	0.00129	3.01 x 10^26
Water	7.4	1.00	3.34 x 10^26
Soft tissue	7.4	1.05	3.36 x 10^26
Fat	5.9-6.3	0.91	3.34-3.48 x 10^26
Bone	11.6 -13.8	1.65-1.85	3.00 - 3.19 x 10^26

Fig. 1. An example of chest radiography

Consider a chest radiographic in Fig.1, this image can be distinguished into three regions: dark region, including majority of lungs; light region with a combination of spine and heart; and gray region containing soft tissue and other sign of pathology.

The rest of this paper is organized as follows. Section 2 presents the method of segmentation, including a recall of pixel-based thresholding method and the proposed method based on the vector of statistical features. In section 3, image data for experiment are expressed, some final results are

Ha Dai Duong is with Faculty of Information Technology, Le Quy Don Technical University (LQDTU), 100 Hoang Quoc Viet, Caugiay, Hanoi, Vietnam duonghadai@yahoo.com

Dao Thanh Tinh is with Faculty of Information Technology, Le Quy Don Technical University (LQDTU), 100 Hoang Quoc Viet, Caugiay, Hanoi, Vietnam tinhdt@mta.edu.vn

978-1-4673-0813-7/12/$31.00 ©2012 IEEE

shown and discussed. Finally, Section 4 gives concluding remarks.

II. Methods

A. Recall pixel-based thresholding

Suppose that the gray-level histogram shown in Fig.2(a) corresponds to an image, F, composed a light object and a dark background, in such a way that object and background pixels have gray levels grouped into two partitions. One obvious way to extract the object from background is to choose a threshold T that separates these partitions. Those pixels which satisfy the condition $f(x,y) > T$ are called object points; otherwise, they are called background points. Fig.2(b) shows a slightly more general case of this approach, where three dominant modes characterize the image histogram. In this case, multilevel thresholding classifies a point (x,y) as belonging to one object class if $T_1 < f(x,y) \leq T_2$, to the other object class if $f(x,y) > T_2$, and to the background if $f(,x,y) \leq T_1$ [8].

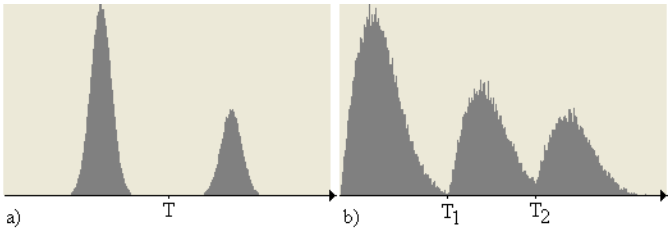

Fig. 2. Gray-level histogram that can be partitioned by (a) a single threshold, and (b) multiple thresholds

Threshold image, G is defined as

$$g(x,y) = \begin{cases} 1 & \text{if } f(x,y) > T \\ 0 & \text{if } f(x,y) \leq T \end{cases} \quad (1)$$

In the case of multilevel thresholding, threshold image, G is defined as

$$g(x,y) = \begin{cases} 1.0 & \text{if } f(x,y) > T_2 \\ 0.5 & \text{if } T_1 < f(x,y) \leq T_2 \\ 0.0 & \text{if } f(x,y) \leq T_1 \end{cases} \quad (2)$$

B. Features vector

In this paper, we propose a new method by replacing the gray-level $f(x,y)$ of each pixel used in the image segmentation method mentioned above with a vector that contains four statistical features that are extracted from the sliding window centred around corresponding pixel. These features are the mean m, the variance v, the third order moment s_3 and the forth order moment s_4 of the window. For an input image F of size $(M \times N)$ and a sliding window of size $(p \times p)$, the four features extracted from the window centred at pixel (x,y) are given by the following equations:

$$m = \frac{1}{p \times p} \sum_{i=-\frac{p-1}{2}}^{\frac{p-1}{2}} \sum_{j=-\frac{p-1}{2}}^{\frac{p-1}{2}} f(x+i, y+j) \quad (3)$$

$$v = \frac{1}{p \times p} \sum_{i=-\frac{p-1}{2}}^{\frac{p-1}{2}} \sum_{j=-\frac{p-1}{2}}^{\frac{p-1}{2}} (f(x+i, y+j) - m)^2 \quad (4)$$

$$s_3 = \frac{1}{p \times p} \sum_{i=-\frac{p-1}{2}}^{\frac{p-1}{2}} \sum_{j=-\frac{p-1}{2}}^{\frac{p-1}{2}} (f(x+i, y+j) - m)^3 \quad (5)$$

$$s_4 = \frac{1}{p \times p} \sum_{i=-\frac{p-1}{2}}^{\frac{p-1}{2}} \sum_{j=-\frac{p-1}{2}}^{\frac{p-1}{2}} (f(x+i, y+j) - m)^4 \quad (6)$$

Note that p must have an odd value to obtain a centred window around each pixel.

Denote $fv(x,y)$, is features vector for pixel (x,y), we define $fv(x,y) = [m, v, s_3, s_4]$. The spatial scanning order of an image is performed, as shown in Fig.3, pixel by pixel from left to right and top to bottom, and a vector of features vector of the image input is generated.

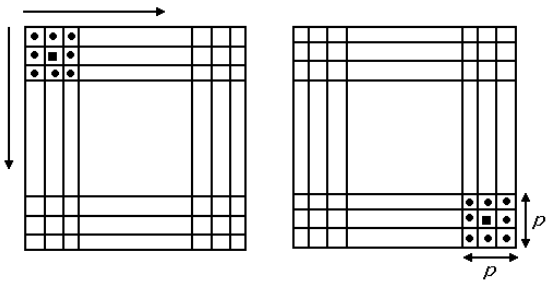

Fig. 3. Features vectors extraction from image

C. Texture-based segmentation

Our proposed method of segmentation is using a schema of multilevel thresholding for features vector as following:

$$g(x,y) = \begin{cases} g_d & \text{if } d(fv(x,y), fv_d) \leq \delta \\ g_g & \text{if } d(fv(x,y), fv_g) \leq \delta \\ g_l & \text{if } d(fv(x,y), fv_l) \leq \delta \end{cases} \quad (7)$$

where $g(x,y)$ is pixel at (x,y) of segmented image G; $d(a,b)$ is the Euclidean distance function from a to b, a and b are points in 4-dimension space; fv_d, fv_g and fv_l are three "centre" points of dark, gray, and light region in 4-dimension respectively; δ is a positive factor. The value of fv_d, fv_g, fv_l and δ will be determined in section III.

III. Experiments

A. Image database

The image database for test in this paper are 40 chest radiographs, they are collected from four Vietnamese national hospital in Hanoi. The images were scanned from films to a size of 400 $\times$ 400 pixels.

TABLE II

REGION'S FEATURE WITH SLIDING WINDOW SIZE OF 9×9

Category	Region	m	v	s_3	s_4
D	D1	52.923	5.178	8.031	10.958
	D2	64.798	5.533	8.519	11.561
	D3	64.031	5.510	8.510	11.577
	D4	71.400	5.718	8.792	11.918
	D5	47.357	4.994	7.781	10.649
	D6	72.632	5.777	8.907	12.095
G	G1	127.980	6.831	10.413	14.023
	G2	113.323	6.598	10.070	13.572
	G3	126.041	6.812	10.382	13.978
	G4	129.442	6.863	10.452	14.066
	G5	122.613	6.759	10.302	13.873
	G6	115.233	6.642	10.131	13.648
L	L1	165.763	7.338	11.128	14.923
	L2	156.852	7.228	10.966	14.709
	L3	167.473	7.359	11.161	14.967
	L4	164.357	7.322	11.105	14.893
	L5	156.565	7.226	10.965	14.710
	L6	153.047	7.182	10.901	14.627

B. Evaluated centre point

Manual segmentation some regions on each image in database into three category: dark regions (D), gray regions (G) and light regions (L). Some regions are taken from image shows in Fig.4. Using set of regions labelled in D, G, L as training set.

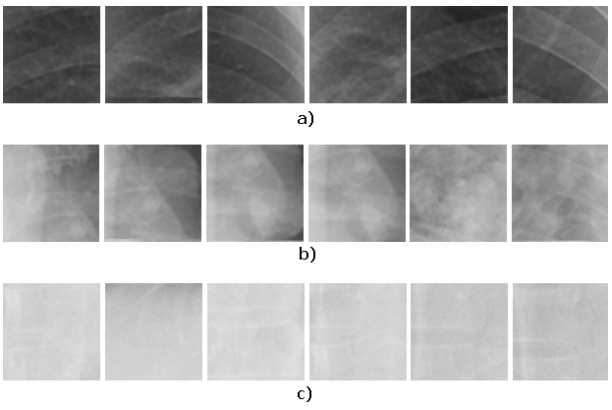

Fig. 4. Image regions are taken from image data, (a) - Dark regions, (b) Gray regions, and (c) Light regions

For each image region in training set, the components m, v, s_3 and s_4 are computed, and then its average vector is carried out. The result for each category D, G and L are given in Table II. Then further averaged over the image regions of each category, the final result shows in Table III.

Now, take the components of centre point equal to each corresponding average feature for dark, gray, and light respectively, we have:

$$fv_d = \begin{bmatrix} 058.093 & 5.328 & 08.254 & 11.250 \end{bmatrix}$$

$$fv_g = \begin{bmatrix} 116.879 & 6.666 & 10.176 & 13.719 \end{bmatrix}$$

TABLE III

CATEGORY AVERAGE FEATURE

Results		m	v	s_3	s_4
D	Average	58.093	5.328	8.254	11.250
	Max	72.632	5.777	8.907	12.095
	Min	44.205	4.875	7.596	10.395
G	Average	116.879	6.666	10.176	13.719
	Max	129.442	6.863	10.452	14.066
	Min	95.007	6.319	9.726	13.190
L	Average	158.623	7.251	11.002	14.759
	Max	167.473	7.359	11.161	14.967
	Min	151.477	7.160	10.868	14.582

$$fv_l = \begin{bmatrix} 158.623 & 7.251 & 11.002 & 14.759 \end{bmatrix}$$

C. Effect of sliding window size

Using the values of p is 3, 7 and 9 respectively, for each value, reconstruct the training set then compute fv_d, fv_g, fv_l, δ and use these values to segment input image by Equ.(7). The experimental results showed that the size 9×9 of sliding window have good performance. For example, in Fig.5 (a), (b) and (c) are segmented images by using our proposed method with $p = 3, 7$, and 9 respectively.

D. Determine the value of δ

Look backward the Equ.(7), obviously the value of δ decides the size of all segmented in dark, gray and light region. If the value of δ is greater then the segmented region will be lager. In this paper, the authors assign the value of δ equal to 1/2 of the minimum distance between each pairs of fv_d, fv_g and fv_l. Rely on the values of fv_d, fv_g, fv_l were computed in previous section, we have: $d(fv_d, fv_g) = 58.885$, $d(fv_d, fv_l) = 100.648$, and $d(fv_g, fv_l) = 41.769$. So that, $\delta \approx 20$.

E. Pixel-based and texture-based methods

The segmented images using multiple pixel-based thresholds with $T_1 = 90$, $T_2 = 180$ and our proposed method are shown in Fig.6. It is obvious that our method outperforms the pixel-based approach. Different regions in the image are clearly partitioned and the resulted image is noiseless.

IV. CONCLUSIONS

In this paper, a new approach to chest radiographs segmentation based on texture features and multilevel thresholding is presented. By using texture feature vector, this approach utilises the information of the pixels in the sliding window to segment, and the experimental results indicate that this method is suitable for chest radiographs. In addition, in the experimental results section, authors have shown calculation methods and a specific case for the determination of centre points and value of threshold. In our approach, the sliding window, particularly its size, plays an important role in the segmentation performance. By recasting the segmentation problem into the statistical space, the proposed method can improve the existing approaches in the literature and therefore enhance the postprocessing tasks like image-based diagnoses.

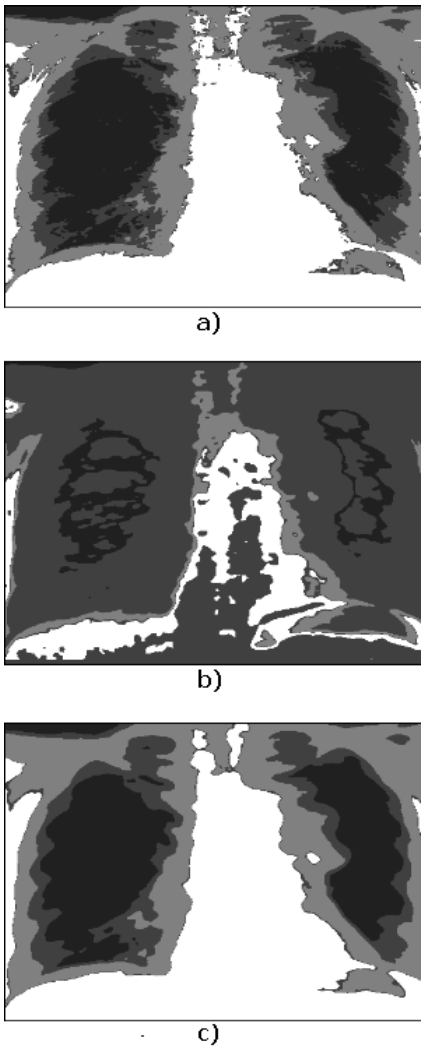

Fig. 5. The segmented images with, (a) p = 3, (b) p = 7, and (c) p = 9

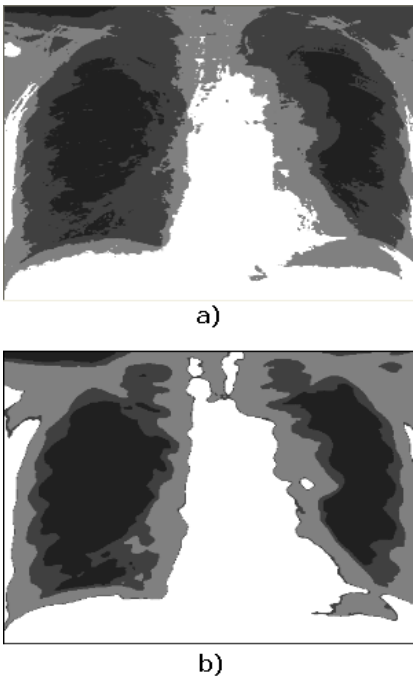

Fig. 6. The segmented images, (a) by pixel-based, and (b) by texture-based method

ACKNOWLEDGMENTS

This work was funded by the Reseach Fund RFit@LQDTU, Faculty of Information Technology, Le Quy Don Technical University.

REFERENCES

[1] Jiann-Shu Lee, Hsing-Hsien Wu, Ming-Zheng Yuan (2009). Lung Segmentation for Chest Radiograph by Using Adaptive Active Shape Models. In Proceedings of the Fifth International Conference on Information Assurance and Security, IAS 2009. pages 383-386.

[2] Ginneken, B.V., Haar Romeny, B.M., Viergever, M.A. (2001). Computer-Aided Diagnosis in Chest Radiography: A Survey. IEEE Trans. Med. Imag. 20(12), pp: 1228-1241.

[3] Alexandros Karargyris, Sameer Antani, George Thoma (2011). Segmenting anatomy in chest x-rays for tuberculosis screening. Engineering in Medicine and Biology Society,EMBC, 2011 Annual International Conference of the IEEE, pp: 7779-7782.

[4] Donia Ben Hassen and Hassen Taleb (2011). A Fuzzy Approach to Chest Radiography Segmentation involving Spatial Relations. IJCA Special Issue on Novel Aspects of Digital Imaging Applications, pp: 40-47.

[5] M. A. Hariyadi, M. H. Purnomo, M. Hariadi, I Ketut E. Purnama (2010). Lung segmentation at image x-ray for detecting cardio-thorax ratio using max-tree filtering and geometry active contour. Journal of Mathematics and Technology, ISSN: 2078-0257, No.4, October, 2010, pp:37-45.

[6] Chhanda Ray, Krishnendu Sasmal (2010). A New Approach for Clustering of X-ray Images. IJCSI International Journal of Computer Science Issues, Vol. 7, Issue 4, No 8, pp: 22-26.

[7] Bruce Hasegawa (1987), Physics of Medical X-Ray Imaging, Medical Physics Pub Corp; 2 edition (June 1987)

[8] Rafael C. Gonzales, Richard E. Woods, Digital Image Processing, Prentice Hall, 2002.